ORIGINAL ARTICLE

Radiologic Patterns of Necrosis After Proton Therapy of Skull Base Tumors

Amine M. Korchi, Valentina Garibotto, Karl-Olof Lovblad, Sven Haller, Damien C. Weber

ABSTRACT: ***Background:*** Discrimination between radiation necrosis and tumor progression after radiation therapy represents a radiologic challenge. The aim of our investigation is to identify patterns of radiation necrosis on brain magnetic resonance imaging (MRI) and positron emission tomography (PET) with Fluoroethyltyrosin (FET) after proton beam therapy (PBT) for skull base tumors. ***Material and Methods:*** Five consecutive patients with extra-axial neoplasms were included, presenting a total of eight radiation necrosis lesions (three clival chordomas; two petroclival chondrosarcomas; two women; mean age: 49 ± 18.2 years). Radiation necrosis was defined as the appearance of abnormal enhancement on MRI after PBT decreasing over time, and additional histopathologic confirmation in one patient. MRI and PET imaging were retrospectively analyzed by two experienced radiologists in consensus. ***Results:*** All lesions were localized close to the primary tumor in the field of irradiation. Three patients showed bilateral symmetrical lesions. All lesions showed T2 hyperintensity and T1 hypointensity. Cerebral blood volume (CBV) was reduced in all available studies. None of the lesions showed a restricted diffusion. FET-PET (three patients) showed a higher uptake in four out of five lesions; three of which had a mean tumor-to-background (TBRmean) uptake lower than 1.95 and FET uptake increasing over time and were correctly classified into radiation necrosis. ***Conclusions:*** Most radiation necroses were in direct continuity with the primary tumor mimicking tumor progression. The most consistent imaging findings for PBT radiation necrosis are low CBV without restricted diffusion and FET-PET TBRmean lower than 1.95 or increasing uptake over time. Bilateral symmetric involvement may be another indicator of radiation necrosis.

RÉSUMÉ: Critères radiologiques de la nécrose après protonthérapie des tumeurs de la base du crâne. ***Contexte :*** La distinction entre la nécrose due à l'irradiation et la progression de la tumeur après l'irradiation est un défi au point de vue radiologique. Le but de notre étude était d'identifier le profil radiologique de la nécrose radio-induite à l'IRM et à la tomographie par émission de positons (PET) à la fluoroéthyltyrosine (FET) après le traitement de tumeurs de la base du crâne par protonthérapie (PT). ***Méthode :*** Cinq patients consécutifs, atteints de tumeurs extra-axiales et présentant au total 8 lésions de nécroses radio-induites, ont été inclus dans l'étude (3 chordomes du clivus, 2 chondrosarcomes pétroclivaux). L'âge moyen des patients était de 49 ± 18,2 ans et 2 étaient des femmes. La nécrose due à l'irradiation était définie par l'apparition d'un rehaussement anormal qui diminuait avec le temps à l'IRM après la PT et par une confirmation histopathologique chez un patient. L'IRM et la PET ont été étudiées rétrospectivement en consensus par deux radiologistes expérimentés. ***Résultats :*** Toutes les lésions étaient localisées dans le champ d'irradiation, près de la tumeur primitive. Trois patients avaient des lésions bilatérales et symetriques. Toutes les lésions présentaient un hypersignal T2 et un hyposignal T1. Le volume sanguin cérébral (VSC) était diminué sur toutes les études disponibles. Aucune des lésions ne présentait une restriction de la diffusion. Le FET-PET de 3 patients montrait une captation plus élevée de 4 lésions sur les 5 imagées. Trois de celles-ci présentaient un rapport moyen de la captation tumorale sur celle du tissu avoisinant (TBRmean) plus faible que 1,95 avec une captation qui augmentait avec le temps; et ont été correctement classifiées comme étant de la nécrose radio-induite. ***Conclusions :*** La plupart des lésions de nécrose due à l'irradiation étaient en continuité directe avec la tumeur primitive mimant une progression de la tumeur. Les critères radiologiques les plus constants de la nécrose due à la PT sont un faible VSC sans restriction de la diffusion et une captation moyenne au FET-PET (TBRmean<1.95) ou augmentant avec le temps. Une atteinte symétrique bilatérale peut être un autre indicateur de nécrose due à l'irradiation.

Can J Neurol Sci. 2013; 40: 800-806

Proton beam therapy (PBT) is used for the treatment of skull base tumors to precisely deliver high-doses of radiation to the tumor volume while sparing normal brain tissue and other organs at risk such as the optic apparatus, the brainstem and the pituitary gland. It offers superior dose distribution as compared to photon radiation therapy. The clinical advantage of PBT over photon techniques is the marked reduction in the integral dose to the patient due to the absence of an exit dose beyond the proton Bragg peak. Proton beam therapy has shown benefits in the treatment of skull base tumors, uveal melanoma, optic pathway gliomas, pituitary adenomas, acoustic neuromas, nasopharynx and paranasal sinus tumors and spinal cord tumors.[1-4].

A rare yet important complication following brain radiation therapy is radiation necrosis[5-7], i.e. the appearance of a new lesion with irregular contrast enhancement, which may mimic a true tumor progression. Radiation necrosis is often seen 3 to 12 months after radiation therapy[6]. Many studies have focused on radiation necrosis following photon radiation therapy for intra

From the Department of Diagnostic and Interventional Radiology (AMK), Department of Nuclear Medicine (VG), Service neuro-diagnostique et neuro-interventionnel DISIM (KOL, SH), Department of Radiation Oncology (DCW), University Hospitals of Geneva, Geneva, Switzerland.

Received February 14, 2013. Final Revisions Submitted May 21, 2013.

Correspondence to: Amine M. Korchi, Department of Diagnostic and Interventional Radiology, Geneva University Hospitals, Rue Gabrielle-Perret-Gentil 4, 1211 Genève 14, Switzerland. Email: mohamed.a.korchi @hcuge.ch.

and extra-axial tumors[5,7,8]. Its incidence after conventional radiation therapy ranges from 5% to 24%[9,10]. The real incidence of radiation necrosis is difficult to assess because of the heterogeneity in the methodology of these studies. For example, different treatment modalities are used and correlation to histopathology is not available throughout. In addition most of these studies were conducted before the widespread use of modern neuroimaging tools[11] and only a few of them assessed radiation injury after PBT[12].

Discrimination between radiation injury and true tumor progression is of paramount importance for further medical care, yet it represents a radiologic challenge. In the current investigation, we aim to describe typical magnetic resonance imaging (MRI) patterns of proton beam therapy induced intra-axial brain necrosis based on a retrospective review of five patients treated by surgery and proton therapy for clival chordoma or petroclival chondrosarcoma. We report results of a relatively new treatment (PBT) for which there is considerably less empirical data compared to "standard" photon radiation therapy.

Methods

Subjects

The local ethical committee approved this study. We retrospectively reviewed MRI and positron emission tomography (PET) examinations of five consecutive cases of necrosis in extra-axial neoplasms between September 2010 and June 2012. We included two patients with petroclival chondrosarcoma (one male and one female) and three patients with clival chordoma (two males and one female). The ages ranged from 28 to 68 years (mean: 49 ± 18.2).

These five patients were treated with PBT at the Paul Scherrer Institut from June 2002 to January 2010, which treated during this time period 73 skull base tumors (42 chordomas and 31 chondrosarcomas). Median administered dose was 74 GyE (range, 68-74). High-energy protons were delivered with a technique of 3 - 4 non-coplanar beams.

The inclusion criterium was appearance of abnormal intra-axial enhancement on T1 gadolinium enhanced MRI after proton beam therapy.

The interval between the start of proton beam therapy and appearance of abnormal enhancement ranged from 9.5 to 42 months (average 26.3 months +/- 14.3). The period of MRI follow-up ranged from 30 to 120 months after proton therapy. Necrosis was confirmed as a decrease in pathologic enhancement in four out of five cases and by surgery followed by histopathology of the surgical specimen in one patient (See Table 1). Fluoroethyltyrosin-PET (FET-PET) was acquired after intravenous administration of 300 MBq of ^{18}F-FET, in one case (patient 5) with a dynamic acquisition from 0 to 40 minutes after injection and in two cases (patients 3 and 4) from 30 to 50 minutes after administration. FET-PET was performed 32, 43 and 77 months after the beginning of treatment for patients 3, 4 and 5, respectively.

Radiological evaluation

Two experienced radiologists retrospectively analyzed in consensus the MRI and FET-PET studies. Since MRI imaging was performed in the context of routine follow-up, MRI protocols were not standardized. Imaging was performed on 1.5 and 3 Tesla routine MRI scanners.

The MRI evaluation criteria were location of the lesions, presence of mass effect and perifocal edema (appearance and signal intensity on T1, T2 and FLAIR sequences), signal intensity on the T2 gradient echo sequence, relative cerebral blood volume (CBV) on Dynamic Susceptibility Contrast (DSC) perfusion imaging, the aspect of enhancement on the T1 gadolinium sequence, the presence of restricted diffusion on Diffusion Weighted Imaging (DWI), and the Chol/NAA ratio on spectroscopy.

The FET-PET evaluation was based on visible uptake (higher than background), on quantitative measures of mean and maximum tumor-to-background (TBRmean and TBRmax) ratio and on the dynamic changes of uptake over time (30 to 40

Table 1: Patient characteristics, radiation therapy information, follow-up period and confirmation of radiation necrosis

Patient number	Diagnosis	Age	Gender	Dose (Gray)	Time between radiation therapy and abnormal enhancement (months)	Follow-up after radiation therapy (months)	Radiation necrosis Confirmation
1	Petro-clival Chondrosarcoma	28y 2m	M	70	9.5	30	Spontaneous decrease of abnormal enhancement
2	Petro-clival Chondrosarcoma	30y 8m	F	70	13	32	Spontaneous decrease of abnormal enhancement
3	Sphenoidal and clival chordoma	57y 6m	M	74	32	38	Spontaneous decrease of abnormal enhancement
4	Clival chordoma	67y 11m	M	74	42	53	Spontaneous decrease of abnormal enhancement
5	Clival chordoma	60y 6m	F	75	35	120	Surgical resection of left temporal lesion

https://doi.org/10.1017/S0317167100015924 Published online by Cambridge University Press

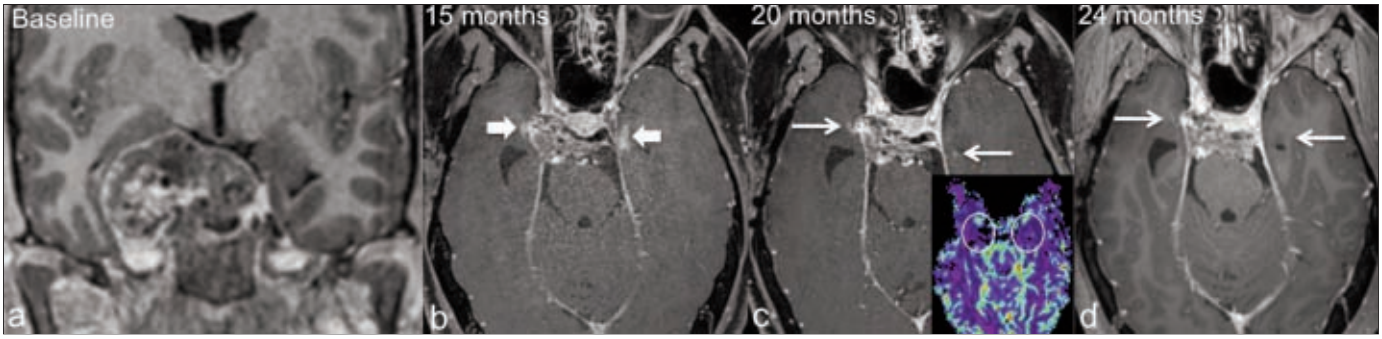

Figure 1: *Patient 1. 28 yo. man with right petroclival chondrosarcoma (a) treated by partial resection followed by proton radiation therapy (70 Gray). MRI follow-up 15 months after the beginning of radiation therapy (b) shows abnormal irregular enhancement (large arrows) in both tempo-medial lobes, adjacent to the residual tumor and within the field of irradiation. Follow-up at 20 and 24 months (c, d) shows decrease and almost complete disappearance of the abnormal enhancement (thin arrows), with a low CBV (circles on image c) confirming the diagnosis of radiation necrosis.*

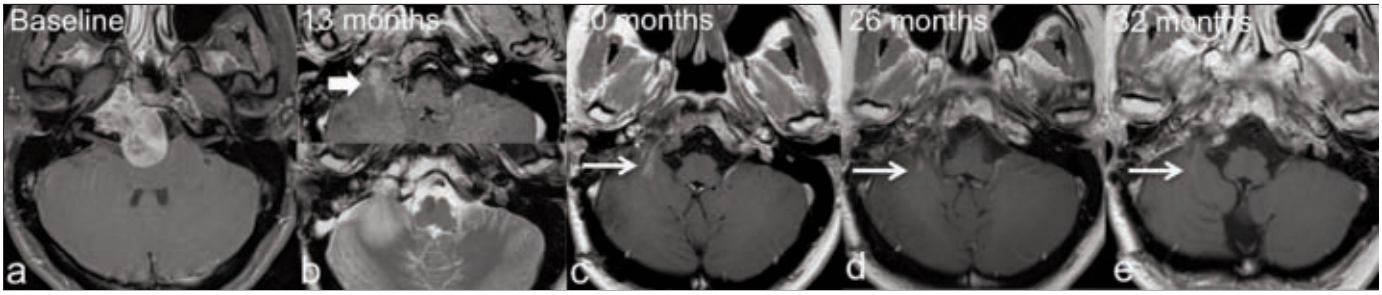

Figure 2: *Patient 2. 30 yo. woman with right petroclival chondrosarcoma (a) treated by surgery and adjuvant proton radiation therapy. On the follow-up MRI, 13 months after initiation of radiation therapy, presence of a new right cerebellar encephalocele through the surgical site with parenchymal edema and heterogeneous enhancement (large arrow, image b). MRI follow-up at 20, 26 and 32 months (c,d,e) shows the resolution of the abnormal enhancement (thin arrows) confirming radiation necrosis*

minutes interval, available for all subjects). The results of these evaluation were expressed as three patterns: increasing over time (Pattern I), stable (pattern II) or decreasing (pattern III), in analogy to the classification recently proposed in an article describing FET-PET features of radiation necrosis after photon radiation therapy[13].

Results

Three patients had two lesions and two patients had one lesion resulting in a total of eight lesions (Figures 1 - 5). Two out of five patients had cardiovascular risk factors. One had controlled high blood pressure and the other was an active smoker (ten pack-year).

One out of five patients was symptomatic, presenting a left third nerve palsy with ptosis and diplopia. These symptoms might have been related with the left temporal necrosis given the spatial proximity between the radiation necrosis and the course of the third cranial nerve. The remaining four patients were asymptomatic.

The clinical course was uneventful for 4 out of the 5 patients included with no clinical or radiological signs of relapse three years (2 patients), four years (1 patient) and ten years and six

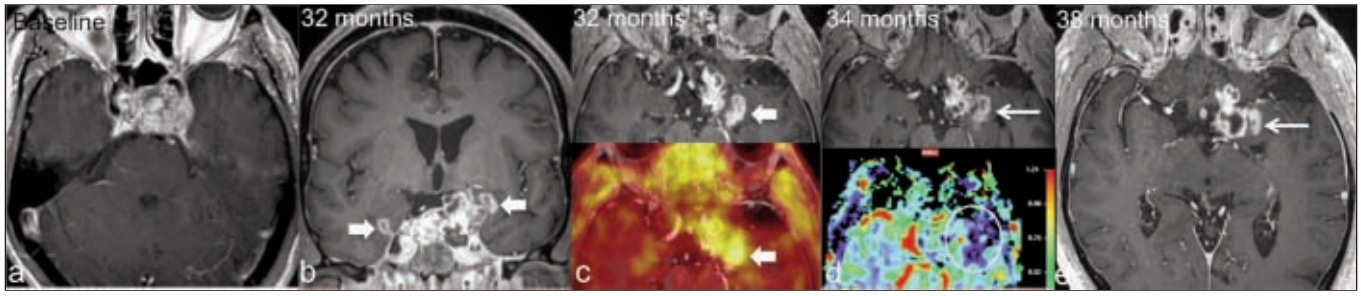

Figure 3: *Patient 3. 57 years-old. man with clival chordoma (a) treated by partial resection and adjuvant proton radiation therapy (74 Gray). On the follow-up MRI, 32 months after the proton therapy, visualization of bilateral abnormal irregular rim enhancement in both temporo-medial lobes (large arrows), showing a significant uptake on FET-PET on the left (large arrow, image c). The lesions are located in both sides of the extra-axial medial primary tumor and within the field of irradiation (b,c). The MRI at 34 and 38 months from radiation therapy shows a spontaneous decrease of the abnormal enhancement (thin arrows, image d and e). The lesions shows low CBV on perfusion MR imaging (circle on image d)*

https://doi.org/10.1017/S0317167100015924 Published online by Cambridge University Press

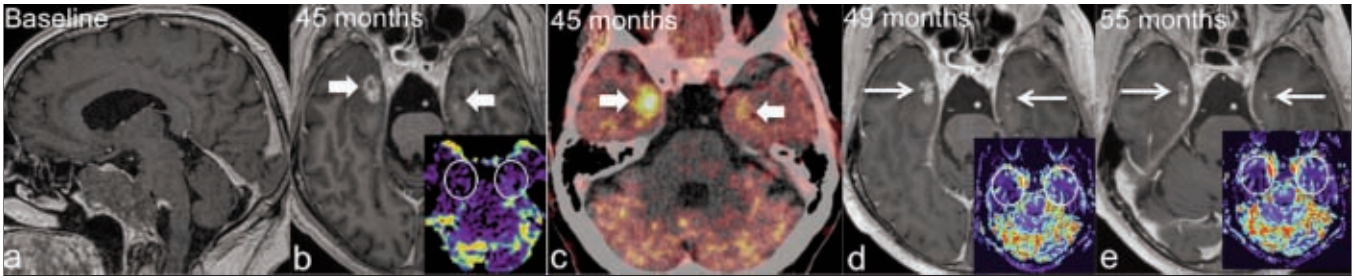

Figure 4: *Patient 4. 68 year-old. man with clival chordoma (a) treated by surgery and followed by proton radiation therapy (74 Gray). MRI done 45 months after the beginning of radiation therapy shows new bilateral abnormal enhancements of the medio-temporal lobes (large arrows, image b); irregular and rim-like on the right, and less pronounced with a nodular, irregular and heterogeneous aspect on the left; the MR perfusion shows no hypervascularisation and a low CBV of the lesions (circles on image b). Both lesions show a moderate uptake on FET-PET (large arrows on image c). Follow-up MRI done at 49 and 55 months shows a decrease of the abnormal enhancement on both sides (thin arrows on images d and e), confirming the diagnosis of radiation necrosis.*

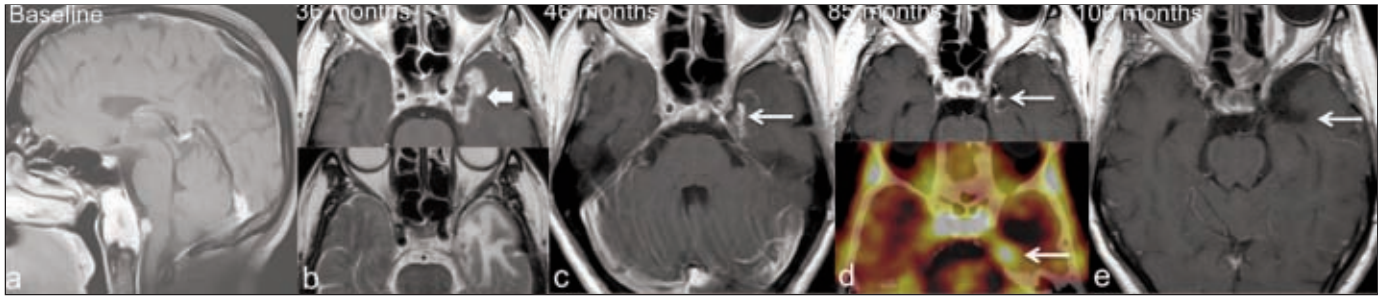

Figure 5: *Patient 5. 60 year-old. woman with clival chordoma extending to the prebulbar space (a) treated by subtotal resection followed by proton radiation therapy (75 Gray). 36 months after the beginning of radiation therapy, MRI follow-up shows new heterogeneous and irregular rim-like enhancement in the left medio-temporal lobe surrounded by edema (large arrow, image b). The MRI at 46 and 85 months (c,d) shows the development of a temporo-polar gliosis and decrease of the abnormal enhancement (thin arrows). The latter has a significant uptake on the FET-PET (thin arrow on image d). The patient subsequently underwent resection of this heterogeneous lesion and the diagnosis of radiation necrosis was confirmed by histopathology. The post-operative MRI, 106 months after radiation therapy (e), shows absence of abnormal enhancement.*

months (1 patient) after the completion of proton therapy. One patient with clival chordoma showed progression of his extra-axial primary tumor four years after the completion of proton therapy, nevertheless without extension to the brain parenchyma. This tumoral progression was seen on the follow-up MRI. Fluoroethyltyrosin-PET was not performed on this occasion for this patient.

Location

In all cases, lesions were localized in close proximity to the primary tumor in the area of irradiation. In three of the five cases, lesions were located in an almost mirror symmetric configuration. In four of the five cases, delineation of radiation necrosis from the primary tumor was not clear, mimicking a continuous lesion.

Although we did not perform a detailed dose-lesion analysis (i.e. brain MRI and computed tomogram (CT) planning fusion), all lesions were in the high-dose (> 90% prescribed dose) region.

Mass effect

Four out of eight lesions presented mass effect. The remaining four lesions were small (<1 cm) without mass effect.

T2 sequence

In all cases, we found hyperintensity with blurry margins, larger than the heterogeneously enhanced area. The signal was homogeneous in one lesion and heterogeneous in the remaining seven lesions found in four patients.

FLAIR sequence

All lesions appeared hyperintense on FLAIR imaging.

T2 gradient echo weighted sequence (T2*)

In two patients, three lesions showed a focal and slight gradient echo T2 hypointensity within the T2 hyperintensity. No abnormality on the gradient echo T2 weighted images (T2*) was seen in the remaining five lesions (3 patients).

T1 sequence

All eight lesions were hypointense on T1W imaging.

Diffusion weighted imaging (DWI)

In one patient, mild hyperintensity on the DWI b1000 was noted in the left temporo-mesial lesion with heterogeneous low signal on the apparent diffusion coefficient (ADC) cartography. In addition, a T2* hypointensity was noted in the same area

https://doi.org/10.1017/S0317167100015924 Published online by Cambridge University Press

corresponding to blood. The abnormal signal on DWI might therefore be related to hemosiderin and not to restricted diffusion. No restricted diffusion was noted in the remaining seven lesions.

Gadolinium enhanced T1 sequence

In four lesions of three patients, irregular rim enhancement was observed. In four lesions of three patients, nodular and heterogeneous enhancement with irregular margins was seen. One patient with lesions in both temporal lobes showed irregular rim enhancement on one side and nodular irregular enhancement on the other side.

Dynamic susceptibility contrast perfusion sequence

In seven lesions of four patients, dynamic susceptibility contrast MRI perfusion showed no hypervascularisation and a decrease in the CBV. Perfusion analysis was not performed on one patient with a unique lesion.

MR Spectroscopy

Spectroscopy was available for three patients. For one patient (patient number 2), the lesion was too small and too close to the skull base for reliable spectroscopy to be performed.

In two patients (patients number 3 and 4), reliable peaks were obtained for NAA and Choline, but not for creatine. Hence we only report the Chol/NAA ratios, which were 1.39 for patient 3 and 1.26 for patient 4.

FET-PET imaging

Fluoroethyltyrosin-PET hybrid imaging was performed for three patients (patients 3 to 5) and showed a visible uptake higher than background in four out of five lesions. For two lesions, the TBRmean and TBRmax values were raised and higher than the cutoff recently suggested for differentiating recurrent brain metastases from radiation necrosis (>1.95 and >2.55, respectively)[13]. Two lesions had an uptake increasing over time (Pattern I), suggestive of radiation necrosis, whereas two lesions had an uptake stable or decreasing (pattern II and III), previously observed for brain metastasis[13]. However, when using the combination of both TBRmean < 1.95 or pattern I as typical for radiation necrosis three of the four lesions showing a visible uptake had FET-PET features previously described in radiation necrosis[13]. Results are summarized in Table 2.

Discussion

In four out of five cases, the radiation necrosis appeared in direct continuity with the primary tumor suggesting tumor progression, which led to biopsy in one case. The intra-axial location became evident only during follow-up imaging, which highlights the importance of being familiar with the imaging characteristics of PBT induced necrosis. The most consistent imaging findings of PBT induced necrosis were hypoperfusion with a low CBV without restricted diffusion. Bilateral symmetric involvement, if present, may be another indicator of PBT induced necrosis.

No lesion presented a restricted diffusion. This finding is in agreement with the study of Kang and colleagues concerning brain metastases treated with radiosurgery, which showed that restricted diffusion with a low ADC value is more likely to be a recurrent tumor. In fact, the latter demonstrates a higher cellularity and less extracellular space available for the protons to move[14,15].

Concerning CBV, our results showing hypoperfusion are concordant with the study by Friso and colleagues in the context of brain metastases after stereotactic radiosurgery. Subjective visual assessment of relative CBV (rCBV) map and a quantitative measurement of rCBV were done on 20 tumor

Table 2: Morphological and functional imaging characteristics of proton beam therapy induced radiation necrosis lesions

Patient number	T2		T1 hypo-intensity	Restricted diffusion	Enhancement		Low CBV	FET-PET				
	Hyperintensity	Mass effect			Rim	Nodular Irregular		Uptake higher than background	TBRmax	TBR mean	Kinetic pattern	Combined analysis of kinetic pattern and TBRmean
Patient 1 Lesion 1	YES	NO	YES	NO	NO	YES	YES	----				
Patient 1 Lesion 2	YES	NO	YES	NO	NO	YES	YES	----				
Patient 2 Lesion 1	YES	YES	YES	NO	NO	YES	YES	----				
Patient 3 Lesion 1	YES	YES	YES	NO	YES	NO	YES	YES	3.3	2.6	Pattern III	Tumor-like
Patient 3 Lesion 2	YES	NO	YES	NO	YES	NO	YES	NO	-	-	-	-
Patient 4 Lesion 1	YES	YES	YES	NO	YES	NO	YES	YES	2.8	2	Pattern I	Necrosis-like
Patient 4 Lesion 2	YES	NO	YES	NO	NO	YES	YES	YES	1.6	1.2	Pattern II	Necrosis-like
Patient 5 Lesion 1	YES	YES	YES	NO	YES	NO	--	YES	1.6	1.2	Pattern I	Necrosis-like

https://doi.org/10.1017/S0317167100015924 Published online by Cambridge University Press

recurrences and 14 tumor necroses suggesting that a high rCBV is associated with tumor recurrence[16]. Our results are also in agreement with the study by Essig and colleagues with 18 patients with brain metastases, showing that a low CBV value is suggestive of treatment response despite the increase in tumor volume probably related to radiation induced modifications[17].

In three out of five cases, lesions were mirror-symmetric. The median-paramedian position of the primary tumors (chordoma and chondrosarcoma) treated by external PBT could be an explanation for the symmetry of the necrosis lesions in both temporal lobes, on both sides of the extra-axial tumor, and within the field of high dose irradiation. By and large, we can assume that the appearance of enhancing lesions on both sides of the proton irradiation target, within the high dose field, is suggestive of radiation necrosis.

In our study, all lesions showed hypersignal on T2W and FLAIR imaging with corresponding hyposignal on T1WI corresponding to perifocal edema. This suggests that these sequences may not be useful for the diagnosis of radio-necrosis. We acknowledge however that this assertion could only be made with a matched cohort of patients with tumor progression.

In our sample, three patients with PBT induced necrosis had FET-PET studies demonstrating a visible uptake in four out of five lesions. The FET-PET positivity despite low CBV values reflects the complex mechanism of tracer uptake, which is influenced by perfusion, blood pool and blood-brain barrier disruption, but also depends on specific amino-acidic transporters in living cells, a measure of cellularity that CBV cannot provide. A positive association between CBV and PET signal has often been reported, but with relevant discrepancies related to the specific processes reflected by the two markers[18].

The presence of a FET-PET uptake higher than background tissue represents a diagnostic challenge. This has also been described in recent reports[19,20] while previous studies indicate that FET-PET can be a valuable tool to detect recurrent tumors[21,22,13]. A recent paper evaluated the performance of FET-PET in differentiating recurrent brain metastases from radiation necrosis, providing a cut-off value for uptake, relative to background (TBRmean and TBRmax) and describing patterns of uptake change over time more suggestive of tumor recurrence or radiation necrosis[13]. Even with the assumption that the recurrence of a skull base chordoma or chondrosarcoma would have a different uptake value and possibly a different dynamic behavior when compared to brain metastases, we tested the robustness of the cutoff proposed in order to verify if the features identified by the authors as "necrosis-like", i.e. a moderately increased uptake as compared with background (lower than 1.95) or an uptake increasing over time, might be an adjunct to image interpretation in these doubtful cases. Importantly, we observed FET-PET features suggestive of radiation necrosis in three out of four lesions with a significant uptake, showing that in the majority of cases, when uptake is visible, quantitative evaluation of this uptake as compared with background and the evaluation of uptake evolution over time can help to correctly classify these patients.

Unfortunately, we could not find FET-PET studies in patients with recurrent skull base chordomas or chordosarcomas in our database or in the current literature. These data would be required to validate the use of quantitative FET-PET measures for the differential diagnosis of recurrent chordoma/chordosarcoma versus radiation necrosis. Given the lack of larger series of patients treated with proton therapy and the absence of FET-PET data in these tumors, FET-PET for this specific indication can only be used in support and association with MRI evaluation and follow-up is ultimately always required. A recent review compared the performance of the various imaging modalities for the differential diagnosis of recurrent glioma vs. radiation necrosis, suggesting that the most sensitive and specific imaging modality was 201-Thallium Single-Photon Emission Computed Tomography (SPECT) with a sensitivity of 87.6% and specificity of 97.8%[23]. Surprisingly, the results of FET-PET studies, yielding a sensitivity and specificity of 92% in a series of 45 patients[24], were not included in the review. No comparative data are yet available concerning the performance of the various imaging modalities for the differential diagnosis of recurrent chordomas or chondrosarcomas versus radiation necrosis.

Proton MR spectroscopy (PMRS) appears to be a valuable tool for differentiating recurrent tumor from radiation necrosis[25,26]. The study by Weybright and colleagues[26] using 2D Chemical shift magnetic resonance (MR) spectroscopy on 16 patients with active tumors and 12 patients with radiation injuries, showed that the Chol/Cr and Chol/NAA ratios were significantly higher, and the NAA/Cr ratio was significantly lower in tumor than in radiation injury. In the latter study, mean values for Chol/Cr, Chol/NAA and NAA/Cr ratios were respectively 2.52, 3.48 and 0.79 for active tumor and 1.57, 1.31 and 1.22 for radiation injury. The primary tumors were intra-axial lesions (glioma, primitive neuroectodermal tumor, medulloblastoma, ependymoma, melanoma and acute promyelocytic leukemia) treated by conventional non-protonic radiation therapy[26]. Since all radiation necrosis lesions in our study were in proximity to the bone, spectroscopy was difficult to perform and Chol/NAA ratio for patients in our sample was in the range of 1.3, which is concordant with the study by Weybright and colleagues.

Limitations

The major limitations of the current study are the small sample size and its retrospective nature, which are due to the relative rarity of radiation necrosis following a therapy which is also infrequent. In addition, follow-up MRI was performed in a clinical setting and therefore MRI protocols were not standardized. Another limitation is that FET-PET had not been performed in two patients and MR perfusion had not been done in one patient. Magnetic resonance spectroscopy was performed in only three out of the five patients.

Conclusion

Our results indicate that hypoperfusion and the absence of restricted diffusion are typically found in radiation necrosis after proton beam therapy for extra-axial neoplasms. If present, bilateral lesions in the region of the irradiation field may be another indicator of PBT induced necrosis. When available, a moderate uptake increase seen in FET-PET or an uptake increasing over time are suggestive of radiation necrosis. Our MRI findings of radiation necrosis after proton beam therapy for extra-axial lesions resemble previous reports of radiation injury following conventional photon radiation therapy for intra-axial

https://doi.org/10.1017/S0317167100015924 Published online by Cambridge University Press

lesions. We therefore conclude that radiation necrosis after proton beam therapy is a process at least partly independent from the underlying pathology, indicating that our findings could be generalized to other primary diseases.

References

1. Khuntia D, Tomé WA, Mehta MP. Radiation techniques in neuro-oncology. Neurotherapeutics. 2009;6(3):487-99.
2. Bouyon-Monteau A, Habrand JL, Datchary J, et al. Is proton beam therapy the future of radiotherapy? Part I: clinical aspects. Cancer Radiother. 2010;14(8):727-38.
3. Brada M, Pijls-Johannesma M, De Ruysscher D. Proton therapy in clinical practice: current clinical evidence. J Clin Oncol. 2007; 10;25(8):965-70.
4. Allen AM, Pawlicki T, Dong L, et al. An evidence based review of proton beam therapy: The report of ASTRO's emerging technology committee. Radiother Oncol. 2012;103(1):8-11.
5. Rogers LR. Neurologic complications of radiation. Continuum (Minneapolis Minn). 2012;18(2):343-54.
6. Brandsma D, Stalpers L, Taal W, Sminia P, van den Bent MJ. Clinical features, mechanisms, and management of pseudo-progression in malignant gliomas. Lancet Oncol. 2008;9(5): 453-61.
7. Shah R, Vattoth S, Jacob R, et al. Radiation necrosis in the brain: imaging features and differentiation from tumor recurrence. Radiographics. 2012;32(5):1343-59.
8. Chen J, Dassarath M, Yin Z, Liu H, Yang K, Wu G. Radiation induced temporal lobe necrosis in patients with nasopharyngeal carcinoma: a review of new avenues in its management. Radiat Oncol. 2011;6:128.
9. Marks JE, Baglan RJ, Prassad SC, Blank WF. Cerebral radionecrosis: incidence and risk in relation to dose, time, fractionation and volume. Int J Radiat Oncol Biol Phys. 1981;7: 243-52.
10. Burger PC, Mahley MS Jr, Dudka L, Vogel FS. The morphologic effects of radiation administered therapeutically for intracranial gliomas: a postmortem study of 25 cases. Cancer. 1979;44: 1256-72.
11. Rahmathulla G, Marko NF, Weil RJ. Cerebral radiation necrosis: A review of the pathobiology, diagnosis and management considerations. J Clin Neurosci. 2013;20(4):485-502.
12. Meyzer C, Dhermain F, Ducreux D. A case report of pseudoprogression followed by complete remission after proton-beam irradiation for a low-grade glioma in a teenager: the value of dynamic contrast-enhanced MRI. Radiat Oncol. 2010;4;5:9.
13. Galldiks N, Stoffels G, Filss CP, et al. Role of O-(2-(18)F-fluoroethyl)-L-tyrosine PET for differentiation of local recurrent brain metastasis from radiation necrosis. J Nucl Med. 2012;53: 1367-74.
14. Kang TW, Kim ST, Byun HS, et al. Morphological and functional MRI, MRS, perfusion and diffusion changes after radiosurgery of brain metastasis. Eur J Radiol. 2009;72:370-80.
15. Asao C, Korogi Y, Kitajima M, et al. Diffusion-weighted imaging of radiation-induced brain injury for differentiation from tumor recurrence. AJNR Am J Neuroradiol. 2005;26:1455-60.
16. Friso W, Hoefnagels FW, Lagerwaard FJ. Radiological progression of cerebral metastases after radiosurgery: assessment of perfusion MRI for differentiating between necrosis and recurrence. J Neurol. 2009;256:878-87.
17. Essig M, Waschkies M, Wenz F, Debus J, Hentrich HR, Knopp MV. Assessment of brain metastases with dynamic susceptibility-weighted contrast-enhanced MR imaging: initial results. Radiology. 2003;228:193-9.
18. Sadeghi N, Salmon I, Decaestecker C, et al. Stereotactic comparison among cerebral blood volume, methionine uptake, and histopathology in brain glioma. AJNR Am J Neuroradiol. 2007; 28(3):455-61.
19. Korchi AM, Garibotto V, Ansari M, Merlini L. Pseudoprogression after proton beam irradiation for a choroid plexus carcinoma in pediatric patient: MRI and PET imaging patterns. Childs Nerv Syst. 2013;29(3):509-12.
20. Garibotto V, Haller S, Vargas MI, et al. Increased uptake of 18F-fluoroethyl-L-tyrosine in radiation-induced brain necrosis (abstract). Eur J Nucl Med Mol Imaging. 2012;39:S382.
21. Rachinger W, Goetz C, Pöpperl G. Positron emission tomography with O-(2-[18F]fluoroethyl)-l-tyrosine versus magnetic resonance imaging in the diagnosis of recurrent gliomas. Neurosurgery. 2005;57(3):505-11.
22. Pöpperl G, Götz C, Rachinger W, Gildehaus FJ, Tonn JC, Tatsch K. Value of O-(2-[18F]fluoroethyl)- L-tyrosine PET for the diagnosis of recurrent glioma. Eur J Nucl Med Mol Imaging. 2004;31(11):1464-70.
23. Shah AH, Snelling B, Bregy A, et al. Discriminating radiation necrosis from tumor progression in gliomas: a systematic review what is the best imaging modality? J Neurooncol. 2013;112(2): 141-52.
24. Pöpperl G, Kreth FW, Herms J, et al. Analysis of 18F-FET PET for grading of recurrent gliomas: is evaluation of uptake kinetics superior to standard methods? J Nucl Med. 2006;47(3):393-403.
25. Taylor JS, Langston JW, Reddick WE, et al. Clinical value of proton magnetic resonance spectroscopy for differentiating recurrent or residual brain tumor from delayed cerebral necrosis. Int J Radiat Oncol Biol Phys. 1996;36:1251-61.
26. Weybright P, Sundgren PC, Maly P, et al. Differentiation between brain tumor recurrence and radiation injury using MR spectroscopy. AJR Am J Roentgenol. 2005;185:1471-6.